International Journal of Nanomedicine

Dovepress
open access to scientific and medical research

Open Access Full Text Article

ORIGINAL RESEARCH

Electrospun polycaprolactone/collagen nanofibers cross-linked with 1-ethyl-3-(3-dimethylaminopropyl) carbodiimide/*N*-hydroxysuccinimide and genipin facilitate endothelial cell regeneration and may be a promising candidate for vascular scaffolds

This article was published in the following Dove Medical Press journal:
International Journal of Nanomedicine

Dian Chen[1]
Tonghe Zhu[2,3]
Wei Fu[4]
Haibo Zhang[1]

[1]Department of Cardiothoracic Surgery, Shanghai Children's Medical Center, Shanghai Jiao Tong University School of Medicine, Shanghai, China; [2]State Key Laboratory for Modification of Chemical Fibers and Polymer Materials, College of Chemistry, Chemical Engineering and Biotechnology, Donghua University, Shanghai, China; [3]Department of Sports Medicine, Shanghai Sixth People's Hospital, Shanghai Jiao Tong University School of Medicine, Shanghai, China; [4]Institute of Pediatric Translational Medicine, Shanghai Children's Medical Center, Shanghai Jiao Tong University School of Medicine, Shanghai, China

Correspondence: Haibo Zhang
Department of Cardiothoracic Surgery, Shanghai Children's Medical Center, Shanghai Jiao Tong University School of Medicine, Dongfang Road, Shanghai, 200127, China
Tel +86 21 3862 5553
Fax +86 21 5090 4612
Email haibo.z@yahoo.com

Purpose: A promising vascular scaffold must possess satisfying mechanical properties, great hemocompatibility, and favorable tissue regeneration. Combining natural with synthetic materials is a popular method of creating/enhancing such scaffolds. However, the effect of additional modification on the materials requires further exploration.

Materials and methods: We selected polycaprolactone (PCL), which has excellent mechanical properties and biocompatibility and can be combined with collagen. Electrospun fibers created using a PCL/collagen solution were used to fashion mixed nanofibers, while separate syringes of PCL and collagen were used to create separated nanofibers, resulting in different pore sizes. Mixed and separated nanofibers were cross-linked with glutaraldehyde (GA), 1-ethyl-3-(3-dimethylaminopropyl) carbodiimide (EDC), and genipin; hence, we named them as mixed GA, mixed EDC (ME), mixed genipin (MG), separated GA, separated EDC (SE), and separated genipin (SG).

Results: Fourier transform infrared (FTIR) spectroscopy and X-ray diffraction showed that cross-linking did not affect the main functional groups of fibers in all groups. ME, MG, SE, and SG met the requisite mechanical properties, and they also resisted collagenase degradation. In hemocompatibility assays, only ME and MG demonstrated ideal safety. Furthermore, ME and MG presented the greatest cytocompatibility. For vascular scaffolds, rapid endothelialization helps to prevent thrombosis. According to human umbilical vein endothelial cell migration on different nanofibers, ME and MG are also successful in promoting cell migration.

Conclusion: ME and MG may be promising candidates for vascular tissue engineering. The study suggests that collagen cross-linked by EDC/*N*-hydroxysuccinimide or genipin facilitates endothelial cell regeneration, which could be of great benefit in tissue engineering of vascular scaffolds.

Keywords: tissue engineering, glutaraldehyde, mechanical test, hemocompatibility, subcutaneous implantation, migration assay

Introduction

Natural and synthetic materials have been used as substitutes or implants in the clinic, including pericardial patches, vascular grafts, and cartilage. Ideal biomaterials

should exhibit cytocompatibility, a low immune response, and appropriate mechanical performances.[1–3] There are many approaches that are used to mimic the extracellular matrix (ECM), which can serve as scaffolds to facilitate cell attachment and supply signals to induce cell migration and proliferation. Collagen is the most abundant protein in the ECM of both soft and hard tissues. It is readily accessible and exhibits great cytocompatibility, such that it is widely used. A high content in the cornea is one reason why collagen has been extensively used in tissue engineering of the cornea.[4] Similarly, collagen scaffolds are widely used in tendon, heart valve, and vascular scaffold repairs.[5–7]

However, collagen is unstable and can rapidly degrade. Therefore, cross-linking treatment is necessary to improve the water resistance of collagen biomaterials. In addition, cross-linking biological tissues can reduce the antigenicity and immunogenicity.[8] Typical cross-linking technologies can be divided into physical, chemical, and biological methods.[9] The major issue with physical methods is that they hardly control the cross-linking density of collagen samples,[10] may not cross-link uniformly,[11] and have the potential to cause damage to DNA (eg, ultraviolet [UV] lighting).[12] The most commonly used chemical cross-linking agents are aldehydes (eg, glutaraldehyde [GA]) and carbodiimides (eg, 1-ethyl-3-(3-dimethylaminopropyl) carbodiimide [EDC]).[13] However, their residual cytotoxicity makes them unsuitable agents to use in tissue regeneration.[14] Genipin, a commonly used biological agent, is generally better tolerated by cells.[15] However, many biological methods are cost-prohibitive. Each cross-linking method results in a different degree of structural and mechanical change. Hence, we elected to compare different cross-linking methods to evaluate their suitability for use with vascular scaffolds.

Although the cross-linking process can enhance the mechanical stiffness of collagen to some extent, the improvement is of limited use in the tissue engineering of vascular grafts for patients with high blood pressure.[16] Polycaprolactone (PCL), which has been approved by the US Food and Drug Administration (FDA) for biomedical applications, is flexible, biodegradable, and biocompatible.[17] Electrospun nanofibers show porosity and a high surface area that facilitates the adhesion, ingrowth, and proliferation of cells.[18] Electrospun PCL/collagen nanofibers are a promising tissue-engineering substitute with great biocompatibility, low cytotoxicity, and excellent tensile strength. PCL/collagen nanofibers, on the other hand, have small pores that could inhibit cell growth into materials.[7] However, collagen can be used to make larger pores as it degrades in vivo. Hence, PCL/collagen nanofibers can be produced using a mixed or separated solution, which results in different pores. In this paper, the effects of different cross-linking technologies for preparing PCL/collagen nanofibers were studied. The mechanical properties, physiochemical characteristics, cytocompatibility, hemocompatibility, and subcutaneous implantation of cross-linked PCL/collagen nanofibers were examined.

Materials and methods

Materials

PCL (Mn =8,000), triton X-100, and paraformaldehyde were supplied by Sigma-Aldrich Co. (St Louis, MO, USA). Collagen, 1-ethyl-3-(3-dimethylaminopropyl)carbodiimide hydrochloride (EDC·HCL), 2-morpholinoethanesulfonic acid (MES), collagenase type I, and penicillin–streptomycin were acquired from Beijing Solarbio Co., Ltd. (Beijing, China). 1,1,1,3,3,3-Hexafluoro-2-propanol (HFIP; purity 99.5%), 2,2,2-trifluoroethanol (TFEA; purity 99.5%), GA (concentration 50%), and *N*-hydroxysuccinimide (NHS) were purchased from Shanghai Aladdin Co., Ltd (Shanghai, China). Genipin (purity 98%) was purchased from Wako Pure Chemical Industries, Ltd. (Osaka, Japan). DMEM/high glucose and PBS were obtained from HyClone Laboratories (Logan, UT, USA). FBS was acquired from Biological Industries Co., Ltd (Kibbutz Beit-Haemek, Israel). 0.25% Trypsin–EDTA was purchased from Thermo Fisher Scientific (Waltham, MA, USA). DAPI was purchased from Enzo Life Sciences (New York, NY, USA). The Cell Counting Kit-8 (CCK-8) was acquired from Dojindo Molecular Technologies Inc. (Rockville, MD, USA). The lactate dehydrogenase (LDH) cytotoxicity assay kit and H&E staining kit were purchased from Beyotime Chemical Reagent (Shanghai, China). All chemicals were used without further purification. Human umbilical vein endothelial cells (HUVECs) were provided by the Shanghai Academy of Life Sciences Cell Bank and Chinese Academy of Science (Shanghai, China). Rats were provided by the Shanghai SLAC Laboratory Animal Co., Ltd. (Shanghai, China). Water used in all experiments was purified using a Milli-Q purification system (EMD Millipore, Billerica, MA, USA).

Preparation of nanofiber membranes

A mixed solution, composed of 10% w/v PCL/collagen (1:1), was dissolved in HFIP. Separate solutions were made of 10% w/v PCL dissolved in TFE or 10% w/v collagen dissolved in HFIP. These solutions were stirred at room temperature for 48 hours. For comparison, two methods were adapted to fabricate membranes. For method 1, a mixed PCL/collagen solution was drawn into a syringe and pumped

Table 1 Electrospinning parameters of mixed and separated nanofibers

Sample	Solvent	Concentration (%)	Flow rate (mL/h)	Distance (cm)	Voltage (kV)	Temperature (°C)	Humidity (%)
PCL/collagen (1:1)	HFIP	10	0.5	12	12–14	20–25	28–35
PCL	TFEA	10	1	9–12	12–14	20–25	28–35
Collagen	HFIP	10	1	9–12	12–14	20–25	28–35

Abbreviations: HFIP, 1,1,1,3,3,3-hexafluoro-2-propanol; TFEA, 2,2,2-trifluoroethanol; PCL, polycaprolactone.

vertically into a drum collector. The electrospun parameters were that the voltage was 12 kV, the distance from needle tip to the collector was 12 cm, and the flow rate was 0.5 mL/h. For method 2, separate PCL and collagen solutions were drawn into separate syringes and electrospun at a flow rate of 1 mL/h, 12 kV high voltage, and a 9–12 cm between the needle tip and the collector. Each electrospun membrane was made with 10 mL of solution (Table 1). All membranes were dried in a vacuum machine for 72 hours to remove the remnant solution. Hence, all membranes were classified as mixed nanofiber or separated nanofiber membranes.

Cross-linking procedures

In this paper, we used three cross-linking technologies: GA, EDC/NHS, and genipin. The collected membranes were put into an enclosed chamber with 25% GA vapor for 24 hours at room temperature.[19] Twenty-five percent of GA solution was prepared from a 50% (v/v) GA stock solution using 95% ethanol as a solvent. In addition, membranes were cross-linked using EDC and NHS. Before cross-linking, membranes were incubated with 0.05 M MES buffer (pH 5.40) for 1 hour and then immersed in 50 mL MES buffer containing EDC and NHS under gentle shaking for 24 hours. A cross-linking solution was made of 2:1 EDC-to-NHS weight ratio using 95% ethanol as a solvent. On the one hand, genipin solution (1 mM) was used to cross-link for 24 hours.[20] After cross-linking, all membranes were rinsed with deionized water and then dried at room temperature for 48 hours. The cross-linked membranes were named as mixed GA (MGA), mixed EDC (ME), mixed genipin (MG), separated GA (SGA), separated EDC (SE), and separated genipin (SG). Fresh membranes were used as the control and were named as fresh mixed membranes (MF) and fresh separated membranes (SF).

Structural and chemical characterizations

Morphological characteristics of the membranes were investigated by scanning electron microscopy (SEM; JSM-5600; JEOL, Tokyo, Japan). Diameters of nanofibers were determined with ImageJ software by randomly selecting 100 data points.

Six membranes were examined with Fourier transform infrared (FTIR) spectroscopy. The spectra were recorded by absorption mode at the 2 cm^{-1} interval in the range of 500–4,000 cm^{-1} using an FTIR spectrophotometer (Nicolet Avatar 380, Thermo Fisher Scientific).

To study the crystal structure of different membranes, X-ray diffraction (XRD) was carried out. The curves were obtained on a D/max-2250 PC X-ray diffractometer (Rigaku Co., Tokyo, Japan) with a scanning region of 2θ (5°–60°). Electrospun PCL membranes and collagen were used as the control.

The water contact angle was used to measure the hydrophobicity of nanofiber membranes. The contact angle was monitored with a video contact angle machine (Attension Theta, Espoo, Finland). Droplets of 0.5 µL were placed on the surface of membranes, and then the contact angle was recorded and automatically calculated at 0, 20, 50, and 90 seconds (n=5).

Mechanical testing

The uniaxial mechanical properties were assessed by applying tensile loads to membranes. Membranes from the eight groups were cut into uniform sizes (4×1 cm, n=4). For comparison, membranes soaked into PBS for 24 hours were set as the control. Both dry and wet membranes underwent mechanical testing. The clips hold two ends of the membranes. With an elongation speed of 10 mm min^{-1}, mechanical properties were tested by a material-testing machine (HY-940FS, Heng Yu Instrument Co., Ltd, Shanghai, China). Ultimate tensile stress (UTS), stress-strain curves, and the elongation at break were determined.

Degradation test of cross-linked membranes

The degradation of nanofiber membranes was measured according to previously published methods.[10,21] In brief, membranes were cut into 1×1 cm^2 and weighed (W_i) and then soaked into degradation solution, which consisted of 1 mL PBS and 12 µg collagenase type I. These membranes were allowed to degrade at 37°C, shaking slowly at 50 rpm. The degradation solution was changed every 3 days. After the selected period of time (1, 3, 5, 10, and 15 days), membranes

were taken out and washed in deionized water twice. The membrane was weighed after thorough drying (W_d). The percentage of weight remaining (W_r) was calculated as follows:

$$W_r = \frac{W_d}{W_i} \times 100\% \quad (1)$$

The results were an average of three independent operations.

On the last time point, the morphological characteristics of different membranes were investigated by SEM.

Hemocompatibility

To assess whether the materials could be used as a vascular substitute, platelet adhesion experiments were conducted. Fresh New Zealand rabbit blood was centrifuged at 1,200 rpm for 10 minutes to obtain platelet-rich plasma (PRP). The different membranes were disinfected and cut into small round pieces and placed in 24-well plates (n=4). Then, 500 μL PRP was added to each well of the 24-well plate. The plate was incubated at 37°C with slow shaking. After 2 hours of incubation, the supernatant was aspirated. Then, the membranes were washed with 37°C PBS three times and transferred to a new 24-well plate. The LDH assay was then performed according to the manufacturer's instructions. The resultant solutions were read at 490 nm using a microplate reader (Multiskan MK3; Thermo Electron Corporation, Waltham, MA, USA), and the mean value of four membranes was calculated.

In addition, biomaterial hemolysis experiments were also carried out. The experimental group (different material leachate), the positive control group (deionized water), and the negative control group (normal saline, NS) were set, and all solutions were prepared in test tubes (n=8). All test tubes were kept in a constant temperature water bath (37°C) for 30 minutes. The anticoagulant-treated fresh rabbit blood and NS were mixed at a ratio of 4:5. 0.2 mL diluted blood was added to each test tube. After that, the test tubes were placed in a constant temperature water bath for 60 minutes and then centrifuged at 3,000 rpm for 5 minutes. Supernatants were retained. The absorbance value was determined at 545 nm, and the mean value of six tubes was taken. The percentage of hemolysis ratio was calculated as

$$D\,(\%) = \frac{(D_t - D_{nc})}{(D_{pc} - D_{nc})} \times 100\% \quad (2)$$

D_t is the absorbance of material leachate, D_{pc} is the absorbance of deionized water, and D_{nc} is the absorbance of NS.

The criterion of hemolysis rate was lower than 5%.

In vitro cell culture

HUVECs were incubated in DMEM with 10% FBS, and 1% penicillin–streptomycin within 5% CO_2. The medium was changed every 3 days. All membranes were put into 24-well plates and soaked in 75% alcohol, sterilizing for 12 hours. DMEM was allowed to infiltrate the membranes before planting cells.

To study the cell viability on different membranes (n=4 for each group), a CCK-8 assay kit was utilized. A density of 2×10^4 HUVECs/well was seeded on the membranes in 24-well plates. At the desired time points of 1, 4, and 7 days, the cell-seeded membranes were processed according to the manufacturer's instructions. The absorbance of each well was measured at 450 nm using a microplate reader.

To observe the morphology of the adhered HUVECs on different membranes, SEM was carried out. A density of 3×10^4 cells/well was seeded on the mats in 24-well plates. The cells and membranes were cocultured for 24 hours, and then the attached cells were fixed with 2.5% GA overnight. Those cells were dehydrated with an ethanol gradient (30%, 50%, 75%, 90%, and 100%) and then dried overnight. Membranes were observed under SEM.

For a substitute of vascular tissue, rapid endothelialization would reduce thrombosis. Hence, the better the ability of cells to move forward horizontally across the material surface, the better the tissue formed. HUVEC migration on different membranes was tested, as previously described.[22] The cells were diluted (1×10^4 cells/well) and placed in sterile Pyrex® cloning cylinders (Thermo Fisher Scientific), which were placed in the center of the membranes for a total of 6 hours. After 6 hours, 500 μL culture medium was added for the desired length of time (0 hour, 24 hours, 4 days, and 7 days) to allow the cells to migrate outward. Then, the membranes were washed with PBS and fixed with 4% paraformaldehyde. The HUVECs adhering to the membranes were stained with DAPI. Then, the stained membranes were imaged by fluorescence microscopy, and the stained HUVECs were quantified using ImageJ software. Every time point had six independent membranes (n=6).

Animal study

All procedures were conducted with respect to the Animal Research: Reporting of In Vivo Experiments guidelines and approved by the Animal Ethics Committees of Shanghai Children's Medical Center, Shanghai Jiaotong University.

In addition, the experiments strictly followed the National Institutes of Health (NIH) Guide for the Care and Use of Laboratory Animals (NIH publications no 8023, revised 1978). To study tissue regeneration in vivo, different membranes were implanted subcutaneously in the backside of rats. Every mixed membrane and separated counterpart (MF and SF, MGA and SGA, ME and SE, and MG and SG) was implanted in the same rat. Upon reaching the designated time point (3, 7, 10, 20, and 30 days), the membranes were removed and fixed with 4% paraformaldehyde. After staining with (immuno)histochemical analysis, the membranes were observed and photographed using a microscope (Leica DMI300B; Leica Microsystems, Wetzlar, Germany). The depth of tissue infiltration was measured with ImageJ software (National Institutes of Health, Bethesda, MD, USA).

Statistical analyses

All results are presented as mean ± SD. The data were analyzed by one-way ANOVA for the evaluation of specific differences. $P<0.05$ was considered statistically significant.

Results and discussion

Fabrication of cross-linked PCL/collagen nanofiber membranes

Nanofiber membranes were fabricated using a mixed PCL/collagen solution with one syringe and separated PCL solution and collagen solution with two syringes. Hence, we referred to these membranes as mixed and separated nanofibers, respectively. To enhance the stability of the PCL/collagen membranes, the fibers were cross-linked with GA vapor, EDC/NHS, or genipin according to the general reaction mechanisms as shown in Figure 1. The morphology of

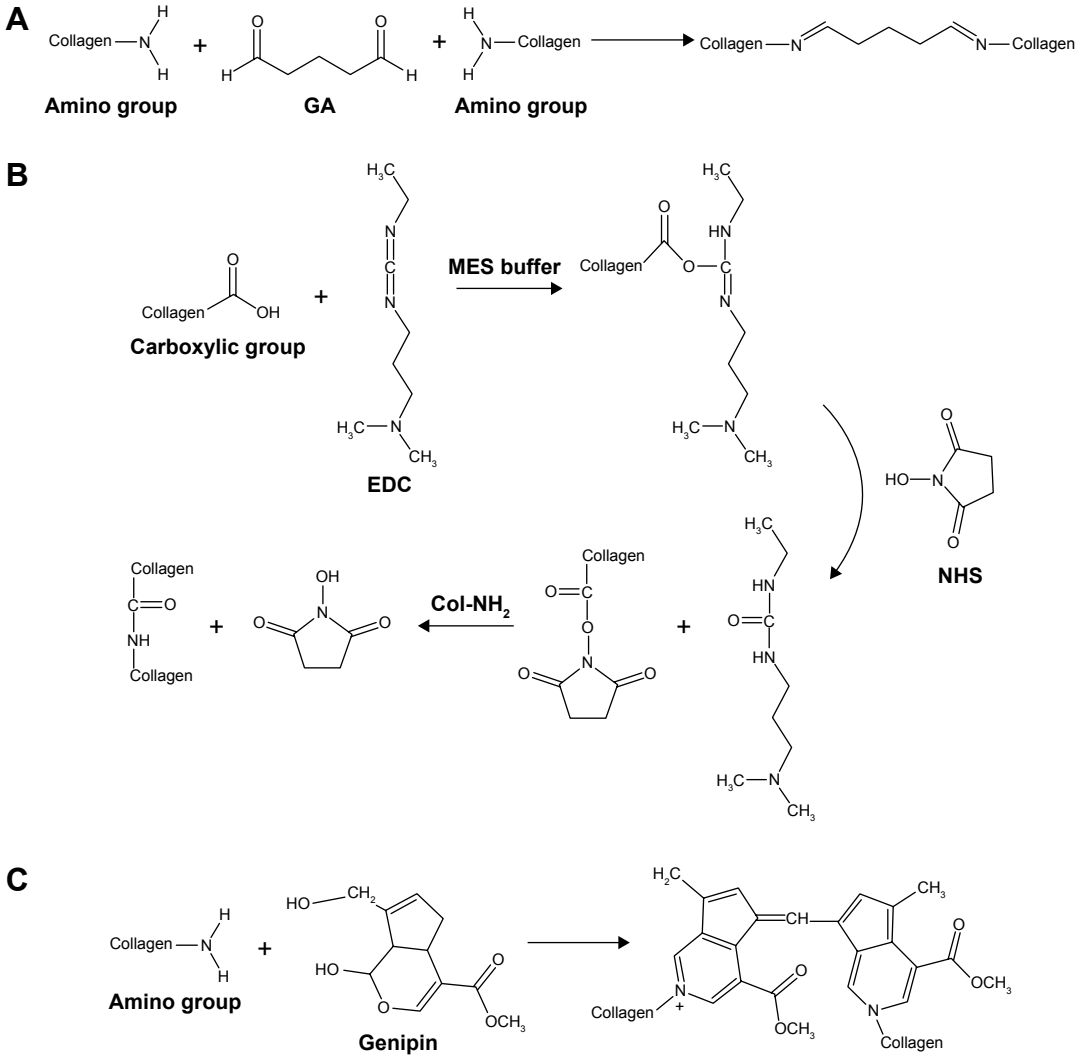

Figure 1 Schematic of the cross-linking reactions of collagen with GA (**A**), EDC/NHS (**B**), and genipin (**C**).
Abbreviations: EDC, 1-ethyl-3-(3-dimethylaminopropyl) carbodiimide; GA, glutaraldehyde; NHS, *N*-hydroxysuccinimide.

these membranes is illustrated in Figure 2A–H. The diameter of MF and SF was 0.16±0.04 μm and 0.37±0.19 μm (Figure 2I and J), respectively. In the mixed nanofibers, fibers were interconnected strongly and twisted, especially the MGA and MG fibers. Accordingly, the pores of the membranes became smaller. After cross-linking, the membranes shrunk to some extent which was reduced by chemical bonds produced within collagen molecules and between different collagen molecules.[23] ME shrunk most severely, followed by MG and then MGA. Creation of aldimine linkages (CH=N) between free amino groups likely explains this change.[24] In other words, genipin could interact with collagen to induce the formation of cyclic structures.[25] In addition, GA promotes collagen stability through the reaction between collagen lysine and hydroxylysine sidechains.[26] The bind composites between collagens treated with EDC/NHS are relatively shorter, which hypothetically causes these membranes to shrink most severely.

In the separated nanofibers, we could see thicker fibers and larger pores than in the mixed nanofibers, which was similar to a previous study.[7] In fact, the diameter of the separated nanofibers was similar to pure PCL fibers,[3] which means the blending of PCL and collagen attenuated the diameter of the fibers. Collagen is a type of polyelectrolyte that can increase charge density.[27] The high charge density on the surface of the solution can increase the voltage between the positive and negative poles, which forces the jet to spray lower diameter fibers. Because PCL fibers and collagen fibers were interspersed with each other in the separated fibers, the appearance of collagen after cross-linking was not obvious.

Chemical and structural characterization of cross-linked membranes

Surface hydrophilicity is an important parameter in tissue-engineering materials. PCL is a hydrophobic material that can be modified by combining it with natural materials,

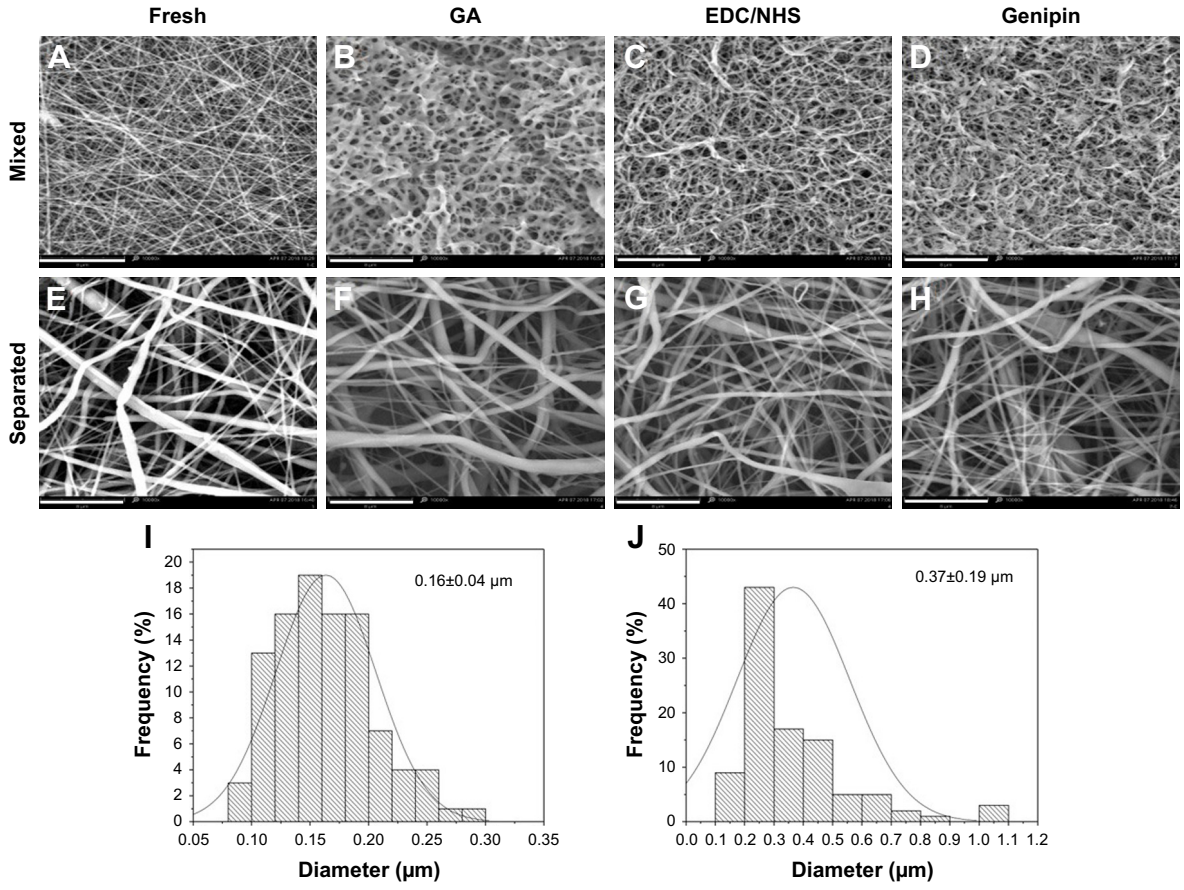

Figure 2 SEM images of different cross-linked membranes under mixed 10% (w/v) solution of PCL/collagen (**A**–**D**) and separated 10% (w/v) PCL and 10% (w/v) collagen solution (**E**–**H**). (**I**, **J**) Fiber diameter distribution of MF and SF, respectively.

Notes: Magnification, 10,000× times. Scale bar, 8 μm.

Abbreviations: EDC, 1-ethyl-3-(3-dimethylaminopropyl) carbodiimide; GA, glutaraldehyde; NHS, *N*-hydroxysuccinimide; PCL, polycaprolactone; SEM, scanning electron microscopy; MF, fresh mixed membranes; SF, fresh separated membranes.

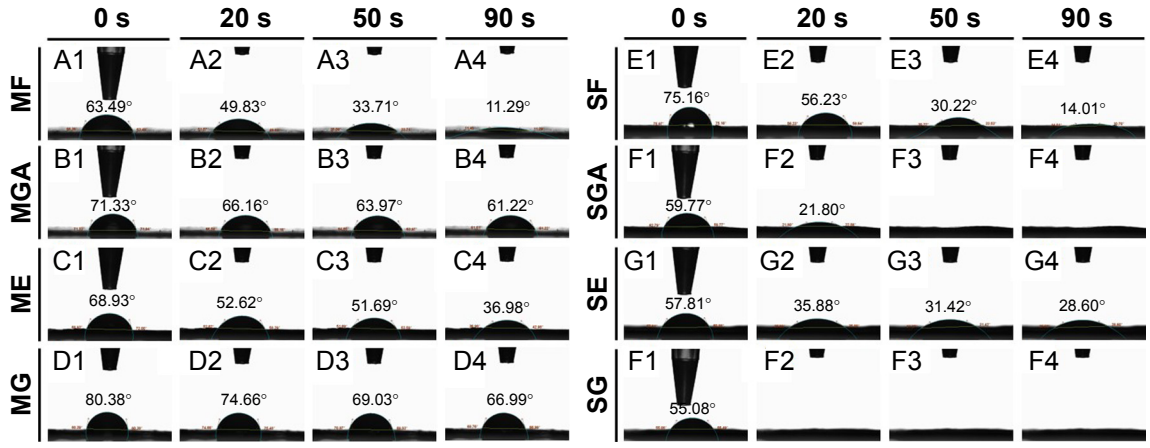

Figure 3 Water contact angles of different cross-linked membranes at desired time points (0, 20, 50, and 90 seconds).
Abbreviations: EDC, 1-ethyl-3-(3-dimethylaminopropyl) carbodiimide; GA, glutaraldehyde; ME, mixed EDC; MG, mixed genipin; MGA, mixed GA; SE, separated EDC; SG, separated genipin; SGA, separated GA; MF, fresh mixed membranes; SF, fresh separated membranes.

such as collagen. As shown in Figure 3, MF and SF were hydrophilic. In the mixed nanofibers, the water contact angles increased after cross-linking, especially in the MGA and MG groups. The results corresponded to the porosity. It is interesting that the hydrophilicity of cross-linked separated nanofibers increased, especially with SGA and SG.[28–30] We hypothesized that the collagen fibers gathered together after cross-linking, increasing the gap between PCL fibers, which augmented the hydrophilicity of the membranes. The changes in the water contact angle may hint that the hydrophilicity of the separated nanofibers was greater than the mixed nanofibers, which was conductive to cell adhesion and growth, at least to some extent.

FTIR is a useful tool to identify the chemical structure of materials. The FTIR spectrum of fresh membranes and different cross-linked membranes is shown in Figure 4. There was no significant difference among the spectrum patterns of different membranes, which means that there were no

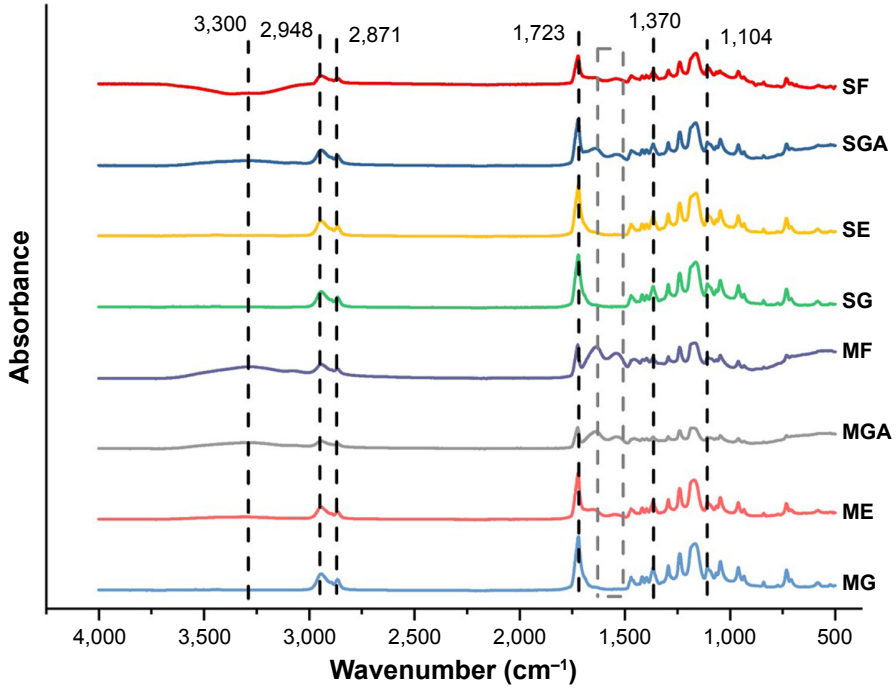

Figure 4 FTIR spectra of fresh and different cross-linked membranes.
Abbreviations: EDC, 1-ethyl-3-(3-dimethylaminopropyl) carbodiimide; FTIR, Fourier transform infrared; GA, glutaraldehyde; ME, mixed EDC; MG, mixed genipin; MGA, mixed GA; SE, separated EDC; SG, separated genipin; SGA, separated GA; MF, fresh mixed membranes; SF, fresh separated membranes.

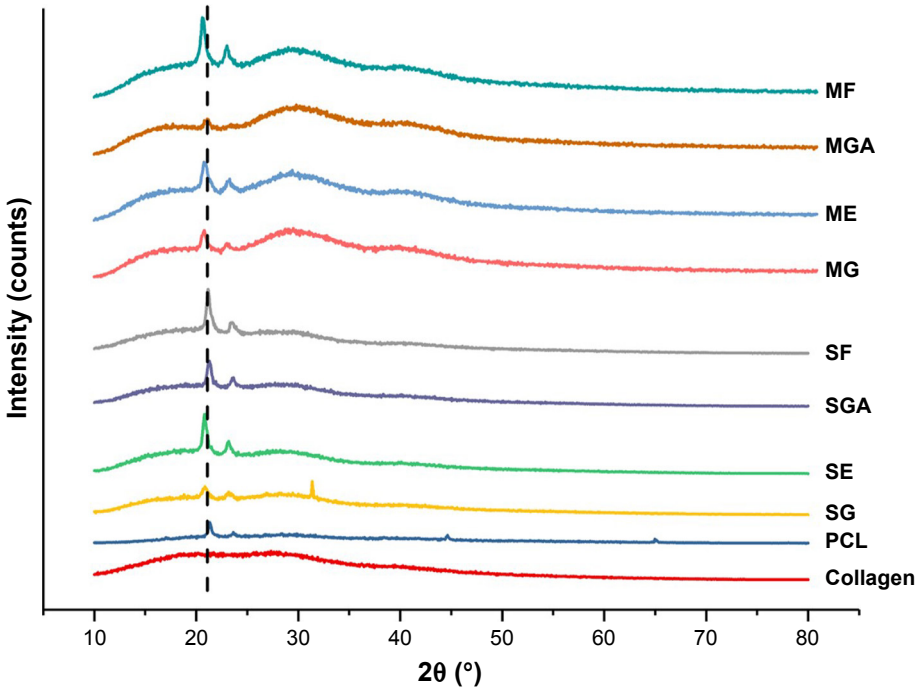

Figure 5 XRD pattern of fresh and different cross-linked membranes.
Abbreviations: EDC, 1-ethyl-3-(3-dimethylaminopropyl) carbodiimide; GA, glutaraldehyde; ME, mixed EDC; MG, mixed genipin; MGA, mixed GA; PCL, polycaprolactone; SE, separated EDC; SG, separated genipin; SGA, separated GA; XRD, X-ray diffraction; MF, fresh mixed membranes; SF, fresh separated membranes.

major changes in the functional groups. In all membranes, the characteristic bands of PCL were found at 2,948 cm^{-1} (asymmetric CH_2 stretching), 2,871 cm^{-1} (symmetric CH_2 stretching), 1,723 cm^{-1} (C=O stretching), 1,294 cm^{-1} (C–C stretching), 1,240 cm^{-1} (asymmetric C–O–C stretching), 1,170 cm^{-1} (symmetric C–O–C stretching), and 1,045 cm^{-1} (C–O stretching).[27,31] As shown in Figure 4, 1,638 cm^{-1} (amide I band), 1,548 cm^{-1} (amide II band), 1,236–1,241 cm^{-1} (amide III band), and 3,300 cm^{-1} (amide A band) bands were also visible, which provided evidence of the presence of collagen.[21] However, these were weak in the membranes cross-linked with EDC/NHS and genipin. The amide I band curves of MGA and SGA were nearly unshifted compared with fresh MF and SF, indicating that the second structure of collagen was not destroyed.[32,33] When collagen is cross-linked with GA, the peak absorbance of the amide III bands increases.[34] On account of the formation of amide bonds between carboxyl groups and available amino groups in ME and SE, the peak of wave numbers at 1,402 cm^{-1} (the symmetric stretching of carboxylate salts), 1,074 cm^{-1} (ester bond), and 2,969 cm^{-1} (CH_2 bond) decreased.[35] The absorbance band at 1,104 cm^{-1} and 1,370 cm^{-1} significantly increased, indicating that collagen was cross-linked with genipin.[12]

XRD can further confirm the crystallinity of materials. Figure 5 shows the XRD patterns of the different membranes. There were two major peaks at 2θ=21.2° and 23.6° in the XRD pattern of PCL, which corresponded to the crystalline nature of PCL.[27] Collagen is an amorphous material that has no obviously sharp peak, rather a broadband at about 2θ=20° in the XRD pattern. We found that the XRD patterns of mixed and separated nanofibers were wider than pure PCL, which indicated the smaller the particles, the broader the diffraction peak.[36] Regardless, in mixed or separated nanofibers, the peak intensities of the cross-linked membranes were shorter than the fresh membranes. We hypothesized that the surface crystalline structures were destroyed by cross-linking agents. Furthermore, there was no significant extra curve or shifted curve, which revealed that cross-linking did not affect the physical structures of the fibers.

Mechanical characterization

To produce tissue-engineering vascular scaffolds, the mechanical strength is integrant. The tensile data of different membranes are presented in Figure 6. In MF and SF, the tensile properties are markedly different between dry and hydrated membranes. Both the UTS and elongation at break were significantly higher in hydrated fresh membranes compared with dry fresh membranes. Furthermore, the difference in the tensile properties of the cross-linked membranes in the hydrated vs dry state was not significant. However, we

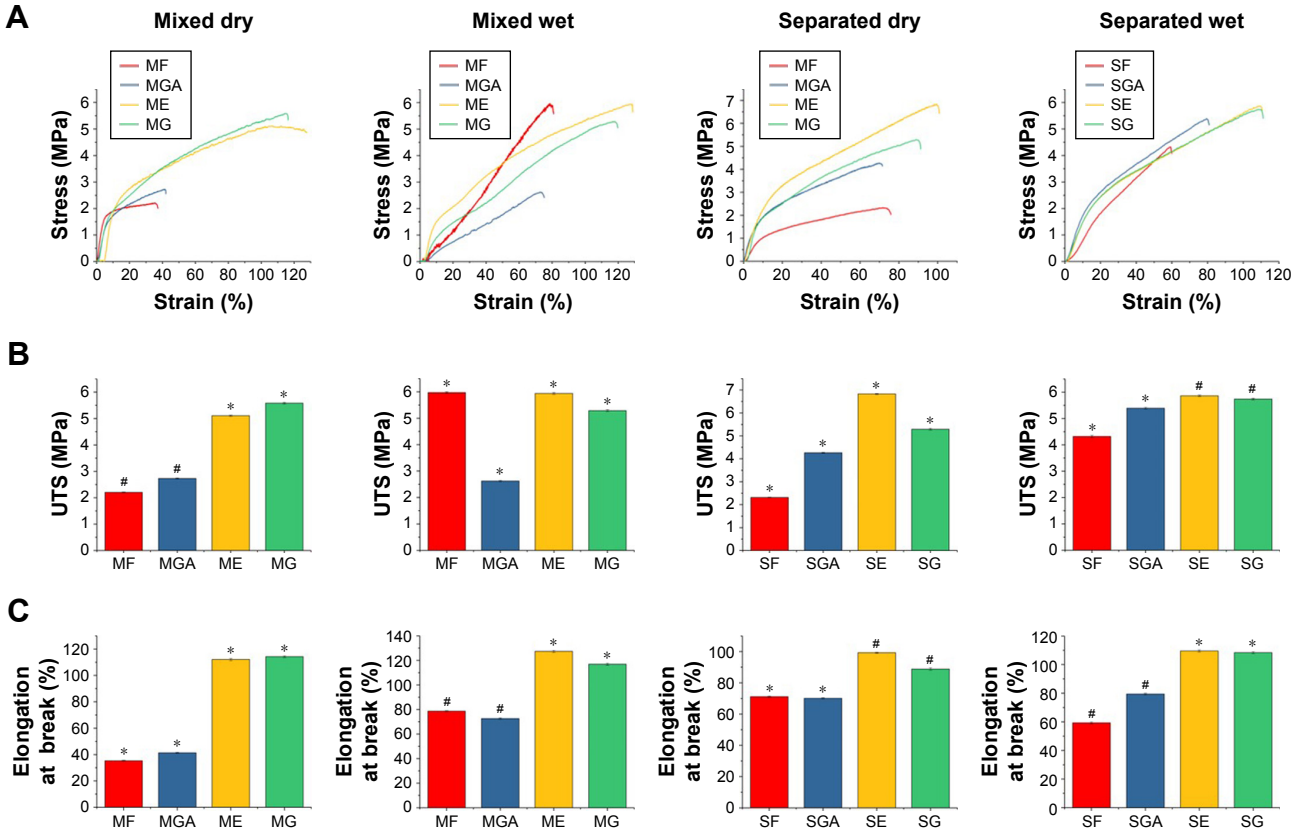

Figure 6 Mechanical assays for different cross-linked membranes.

Notes: (**A**) Curve of stress on tensile process. (**B**) UTS. (**C**) Elongation percentage on the break of tensile process. *A statistically significant difference for the mean value compared with all other membranes. #Denotes a statistically significant difference for the mean value compared with other membranes except the group with the same # symbol ($P<0.05$, n=4).

Abbreviations: EDC, 1-ethyl-3-(3-dimethylaminopropyl) carbodiimide; GA, glutaraldehyde; ME, mixed EDC; MG, mixed genipin; MGA, mixed GA; SE, separated EDC; SG, separated genipin; SGA, separated GA; UTS, ultimate tensile stress; MF, fresh mixed membranes; SF, fresh separated membranes.

found that the tendency of the mechanical curve of hydrated cross-linked membranes was relative to hydrophilicity. PCL is a hydrophobic material, and there is little difference in the mechanical properties between the dry and wet state.[37] Collagen has a natural tendency to absorb fluid, which increases its flexibility.[38] Furthermore, the carbonyl, carboxyl, and hydroxyl groups of the fibers in water would form a hydrogen bond that strengthens the mechanical properties of the fibers,[39] as evidenced by the UTS and elongation at break. However, the elongation of SF decreased after hydration, and we suspect that irregular degradation of the collagen is responsible. Even so, whether the mechanical effects of collagen addition to PCL are positive or negative remains controversial.[27,37] Both the physical and chemical bonds between fibers would affect the mechanical properties. Under different cross-linking mechanisms, concentrations, and exposure time, each cross-linking technology presents different degrees of structural and mechanical stability.[13] Considering the mechanical properties of the porcine coronary artery, the UTS was 2.6 MPa and the elongation was 100%.[37] In our study, only ME, MG, SE, and SG meet the abovementioned two requirements simultaneously. GA-fixed membranes performed poorly with other cross-linked counterparts, which corresponded to a previous study.[25]

In vitro enzymatic degradation of cross-linked membranes

Ideal tissue-engineering materials should be biodegradable. As these materials degrade, the neo-tissue grows into the materials. Hence, the materials should possess an ideal degradation rate. PCL degrades in vivo on a magnitude of years, while collagen degrades fast, which possibly results in the crystalline form of the materials.[40] Figure 7A depicts that separated cross-linked fibers were degraded faster than mixed cross-linked ones, which was related to the pore diameters and surface hydrophilicity. Separated cross-linked fibers possessed larger pores, which induced larger contact surface area with degradation solution. Figure 7B depicts the

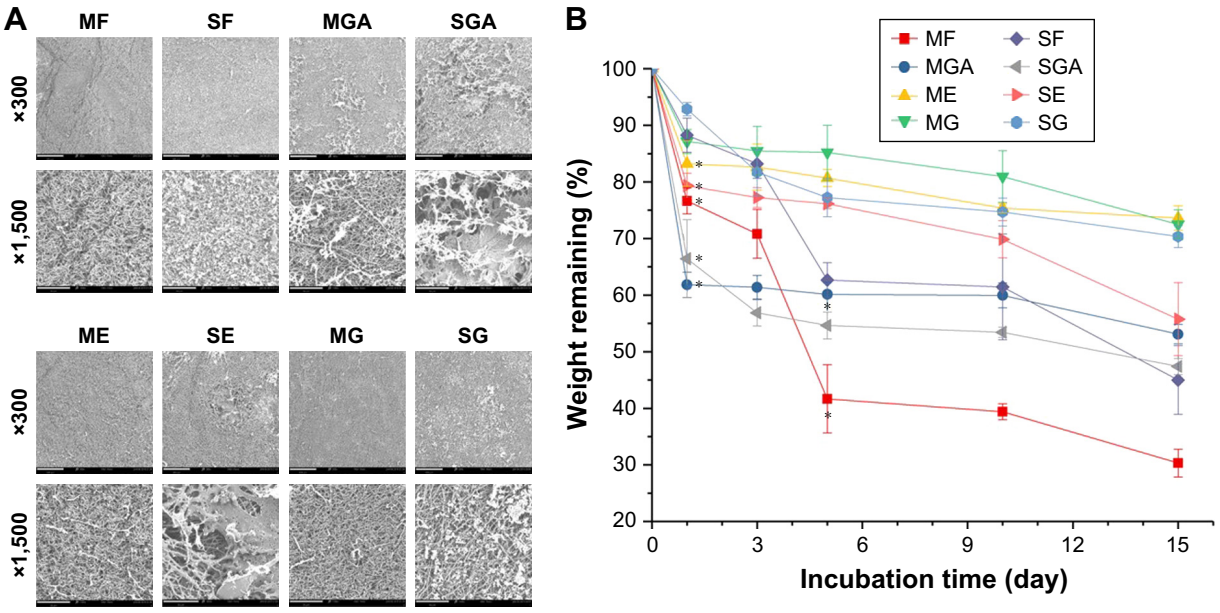

Figure 7 Degradation test for different cross-linked membranes.
Notes: (**A**) SEM images of different cross-linked membranes after soaked in degradation solution on the 15th day. Magnification, 300× times; scale bar, 200 μm. Magnification, 1,500× times; scale bar, 50 μm. (**B**) Weight remaining in different cross-linked membranes after incubating at 37°C in PBS with collagenase type I. *A statistically significant difference ($P<0.05$, n=4) in the mean value compared with the last time point.
Abbreviations: EDC, 1-ethyl-3-(3-dimethylaminopropyl) carbodiimide; GA, glutaraldehyde; ME, mixed EDC; MG, mixed genipin; MGA, mixed GA; SE, separated EDC; SEM, scanning electron microscopy; SG, separated genipin; SGA, separated GA; MF, fresh mixed membranes; SF, fresh separated membranes.

weight remaining of different membranes soaked in PBS and collagenase at the designated time points (1, 3, 5, 10, and 15 days). MF and SF degraded the most. Interestingly, we found that the degradation of MF did not correspond to the concentration ratio of the solution. In other words, the ratio of the mixed solution was composed of PCL and collagen at a 1:1 ratio, while the degradation of MF over a relatively short span of time was about 70%. Previous studies have indicated that several enzymes, such as protease and lipase, can accelerate the degradation of scaffolds.[41] The addition of collagen would be expected to result in discontinuity of the PCL fibers. In the case of collagenase, the fast degradation of collagen would create defects in the fibers. Accumulated defects break the structure of the fibers, leading to faster degradation. As shown in Figure 7, after cross-linking with genipin or EDC/NHS, the resistance of the membranes against collagenase degradation significantly increased. The cleavage site of collagen was covered or masked by cross-links with genipin or EDC/NHS with free amino acids, which inhibited the enzyme–structure response, resulting in an altered degradation rate.[10,25]

In vitro cell viability

In vitro cell viability tests were used to primarily detect whether the membranes meet the fundamental cytocompatibility requirements in tissue engineering. Vascular endothelial cells play critical roles in maintaining vascular functions. In our study, HUVECs were used. The proliferation of HUVECs on days 1, 4, or 7 after culture is presented in Figure 8A. Compared with the blank coverslips, cell viability on MF, ME, and MG was unchanged. However, the cell viability on MGA and SGA was significantly lower than the others on day 7. GA is an efficient cross-linking agent. However, the residual cytotoxicity of the GA-treated membranes renders it very cytotoxic.[42] The high cytotoxicity of GA may result from the fact that this agent is subject to polymerization. Aldehyde groups of GA undergo nucleophilic substitution by adding amines, thiols, and imidazoles to the cell, thus inducing toxicity.[21] In the process of cross-linking, EDC/NHS does not enter the structure of the products, but produces the by-product urea.[43] Therefore, EDC/NHS is also considered to have little potential toxicity. To avoid the cytotoxic effects of chemical agents, biological methods have also been assessed. Genipin has received attention for its excellent biocompatibility. It has been reported previously that genipin has much less cytotoxicity than GA. Moreover, residues released from the membranes cross-linked by genipin were non-cytotoxic.[25] Nevertheless, the cytotoxicity of genipin is related to its concentration. Under the premise of ensuring cross-linking efficiency, the concentration of genipin should be limited to less than 1 mM.[12] Generally, large pores between the fibers facilitate cell infiltration and nutrient flow between cells. On the other hand, although smaller diameter fibers are so dense that cells have difficulty in infiltrating them, they

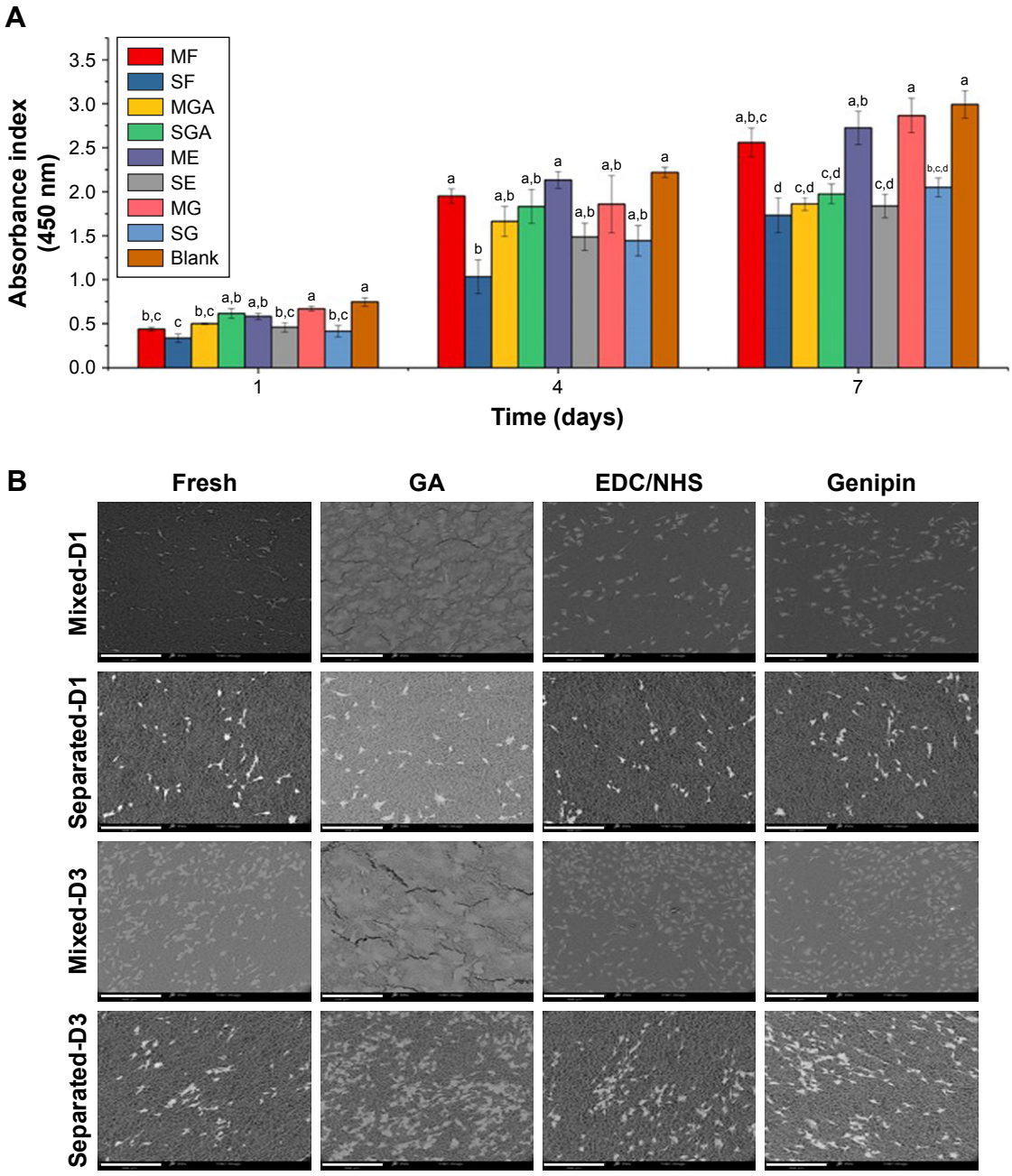

Figure 8 (**A**) CCK-8 assay of HUVEC proliferation adhered on the coverslips and different cross-linked membranes at desired time points (1, 4, and 7 days after operation). The sequence of letters a–d represents the size of the mean value (a>b>c>d). The same letter indicates no statistically significant difference ($P<0.05$, n=4). (**B**) SEM observations of HUVECs grown on the different cross-linked membranes at 1 and 4 days after culture. Magnification, 250×. Scale bar, 300 μm.

Abbreviations: CCK-8, Cell Counting Kit-8; EDC, 1-ethyl-3-(3-dimethylaminopropyl) carbodiimide; GA, glutaraldehyde; HUVECs, human umbilical vein endothelial cells; ME, mixed EDC; MG, mixed genipin; MGA, mixed GA; NHS, *N*-hydroxysuccinimide; SE, separated EDC; SEM, scanning electron microscopy; SG, separated genipin; SGA, separated GA; MF, fresh mixed membranes; SF, fresh separated membranes.

provide more attachment points for the cells. However, large diameter fibers with wide gaps do not permit cell adhesion across neighboring fibers.[44] Adhesion behaviors of HUVECs on the different membranes were evaluated by SEM on days 1 and 4 (Figure 8B). HUVECs exhibit good adhesion to the surface of nanofiber membranes. Compared with day 1, the number of cells adhering to the membranes increased significantly on day 4, indicating that cell proliferation was an upward trend. Particularly, the HUVECs on ME and MG proliferated the fastest, and the results were consistent with the results of the CCK-8 assays.

Platelet adhesion and hemocompatibility

Since the designed nanofiber membranes are used in vascular tissue engineering, it is important to investigate their hemocompatibility. Materials with high hemolysis activity not only cause the destruction of red blood cells leading to diseases, such as anemia, but also aggravate the aggregation

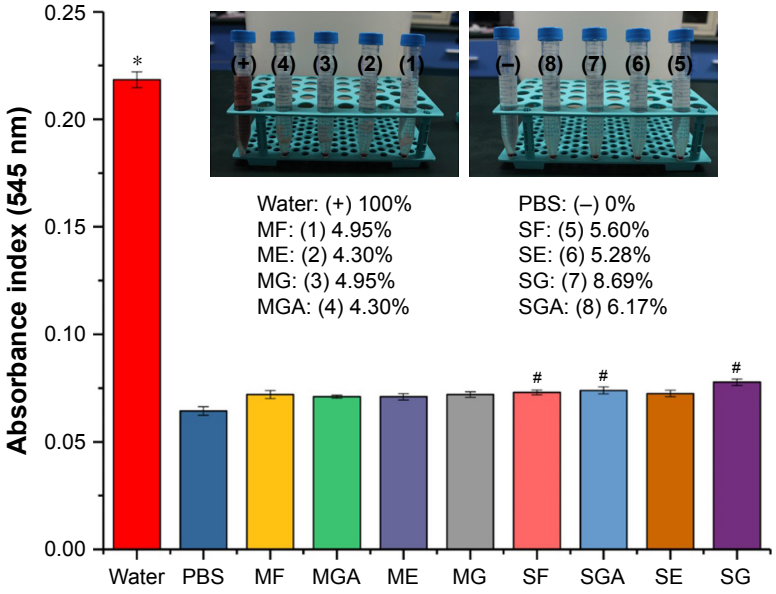

Figure 9 Hemolytic assay of different cross-linked membranes.
Notes: *A statistically significant difference in the mean value compared with all other membranes. #Denotes a statistically significant difference in the mean value compared with water and PBS ($P<0.05$, n=8).
Abbreviations: EDC, 1-ethyl-3-(3-dimethylaminopropyl) carbodiimide; GA, glutaraldehyde; ME, mixed EDC; MG, mixed genipin; MGA, mixed GA; SE, separated EDC; SG, separated genipin; SGA, separated GA; MF, fresh mixed membranes; SF, fresh separated membranes.

of platelets via ADP released by lysed erythrocytes, which leads to thrombosis.[45] For comparison, distilled water was designated as the positive control, while PBS served as the negative control. As shown in Figure 9, with the exception of the positive control and the separated membranes, the hemolysis rates of the negative control and the mixed membranes were <5% (the safe value). On the other hand, membranes treated with EDC/NHS presented relatively low hemolytic activity, regardless of whether they were mixed or separated membranes.

Figure 10 shows the quantitative statistics of platelet deposition on different membranes. The platelet deposition

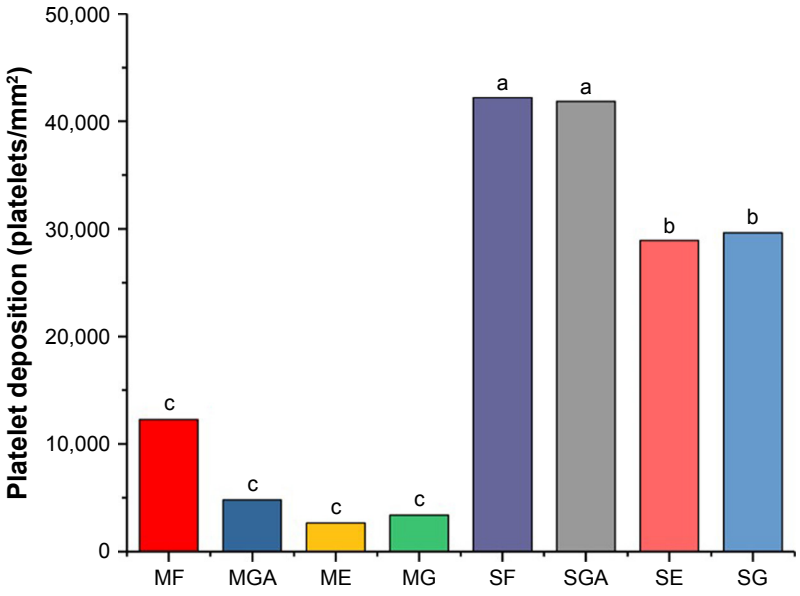

Figure 10 Platelets deposited on different membranes, quantified by LDH activity.
Notes: The sequence of letters a–c represents the size of the mean value (a>b>c). The same letter indicates no statistically significant difference ($P<0.05$, n=4).
Abbreviations: EDC, 1-ethyl-3-(3-dimethylaminopropyl) carbodiimide; GA, glutaraldehyde; LDH, lactate dehydrogenase; ME, mixed EDC; MG, mixed genipin; MGA, mixed GA; SE, separated EDC; SG, separated genipin; SGA, separated GA; MF, fresh mixed membranes; SF, fresh separated membranes.

of SF and SGA was most severe (greatest number adhering), and there was no significant difference between these two groups. Compared with that, the deposition levels on mixed membranes were significantly decreased. Although there was a similar level of platelet deposition among mixed membranes, it appeared that fewer platelets adhered to ME and MG. Collagen was one of the primary targets for nonselective cell adhesion proteins.[46] However, this affinity was not merely to the endothelial cells but also to other components that exist in blood, such as platelets.[47] Hence, collagen possesses pro-thrombogenic properties, but fixation can change the primary structure of collagen and reduces platelet adhesion to some extent.

Inflammatory response

Figure 11 shows the immunohistochemical analysis within CD45 and CD163 of different cross-linked membranes after subcutaneous implantation on the 10th day, which represented early stage of host responses to the implantation. CD45 (+) leukocyte largely presented in MGA and SGA, and barely in other groups. CD163 (+) M2 macrophage presented in SGA and SG. Implantation of synthetic materials could evoke an inflammation reaction dominated by neutrophils and macrophages.[48] M1 macrophage is a key effector cell in foreign body reaction, while M2 macrophage facilitates tissue regeneration. A mixed M1/M2 phenotype in SGA indicated that both a constructive and destructive tissue formation were present in the host immune responses. It was known that the reduction in free amino groups in biological tissue could diminish its antigenicity.[49] The abnormality in GA-fixed membranes was supposed in pro-inflammatory effects on macrophage-like cells and disrupted host tissue remodeling.[50]

Migration assay

The integrity of the intima of the blood vessels prevents thrombosis and serves to maintain the patency of blood vessels. It is agreed that the endothelium plays a critical role in the regulation of vascular hemostasis. Some studies have shown that angiogenic endothelial cells are remolded by endothelial progenitor cells in blood,[51] while others have shown that normal endothelial cells at both ends migrate to the middle to regenerate the endothelial layer.[52] Therefore, we tested the ability of HUVECs to migrate against the membrane surface. A certain number of HUVECs were planted in a hollow cylinder and cultured for a period of time to migrate outward. At the desired time points (0 hour, 1, 4, and 7 days), we fixed the cells and stained with DAPI. In Figure 12, the migration of cells on the surface of different

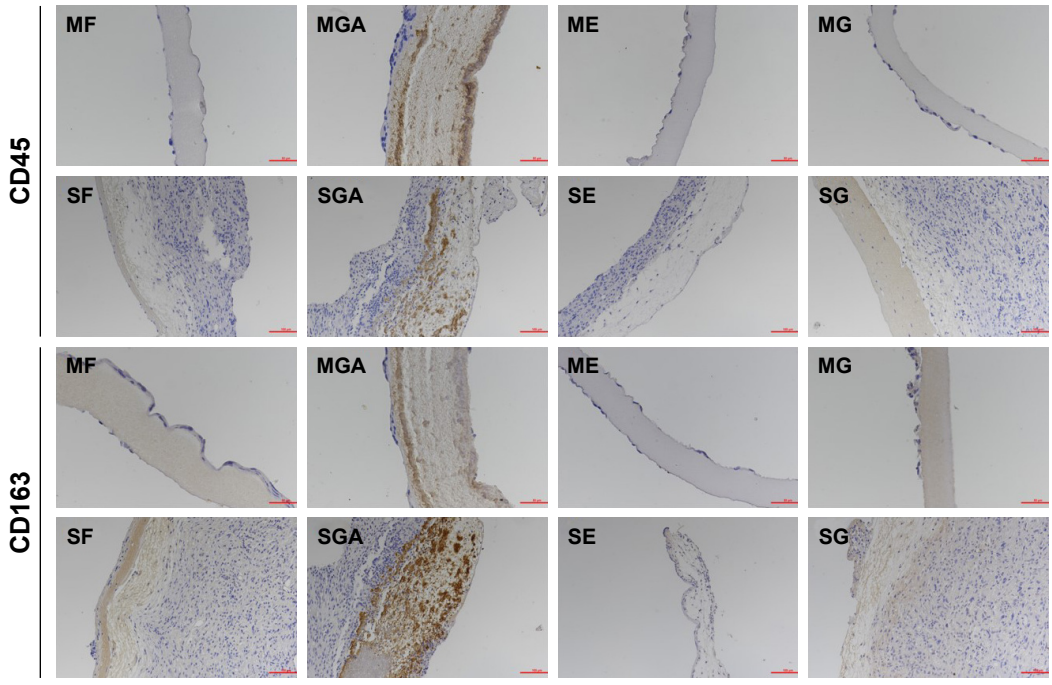

Figure 11 Cross-sections within immunohistochemical analysis of different cross-linked membranes after subcutaneous implantation.
Notes: The scale bar of first and third line, 50 μm. The scale bar of second and last line, 100 μm.
Abbreviations: EDC, 1-ethyl-3-(3-dimethylaminopropyl) carbodiimide; GA, glutaraldehyde; ME, mixed EDC; MG, mixed genipin; MGA, mixed GA; SE, separated EDC; SG, separated genipin; SGA, separated GA; MF, fresh mixed membranes; SF, fresh separated membranes.

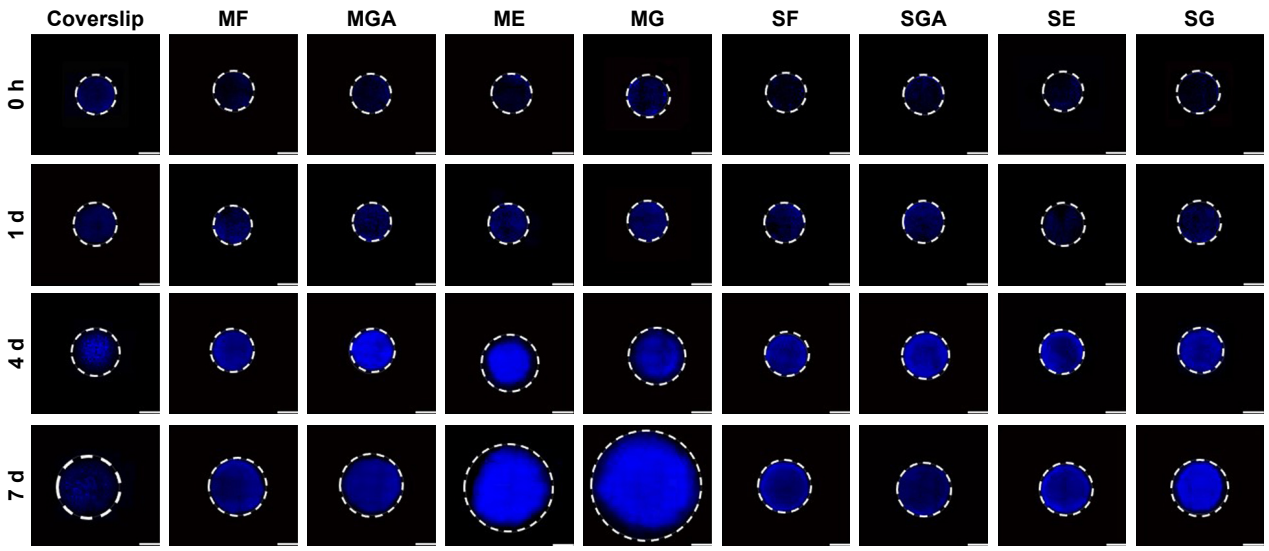

Figure 12 Migration of HUVECs on the coverslips and different cross-linked membranes with DAPI staining at desired time points (0 hour, 1 day, 4 days, 7 days). Scale bar, 4,000 μm.
Abbreviations: EDC, 1-ethyl-3-(3-dimethylaminopropyl) carbodiimide; GA, glutaraldehyde; HUVECs, human umbilical vein endothelial cells; ME, mixed EDC; MG, mixed genipin; MGA, mixed GA; SE, separated EDC; SG, separated genipin; SGA, separated GA; MF, fresh mixed membranes; SF, fresh separated membranes.

membranes is shown. The white dashed boxes measure the furthest outward migration of HUVECs and draw a circle with that distance as the radius. The HUVECs migrated more rapidly on coverslips, ME, and MG compared with the other nanofiber membranes. The cell migration distance was furthest on MG. However, separated membranes did not show a consistent migration pattern over increasing time.

The cell coverage area and outward migration percentage after HUVECs were cultured over 7 days were computed (Figure 13). Over 7 days of migration, there was no significant difference between ME, MG, and coverslips. Compared with them, the migration rates of MF, MGA, SF, SGA, SE, and SG were lower. Obviously, the migration rates on mixed membranes were higher than on separated membranes. It has been proposed that cell contact guidance effects would influence cell behavior, indicating cell proliferation and migration. Generally, the diameter of fibers can affect the cellular adhesion contact point.[53] This may be

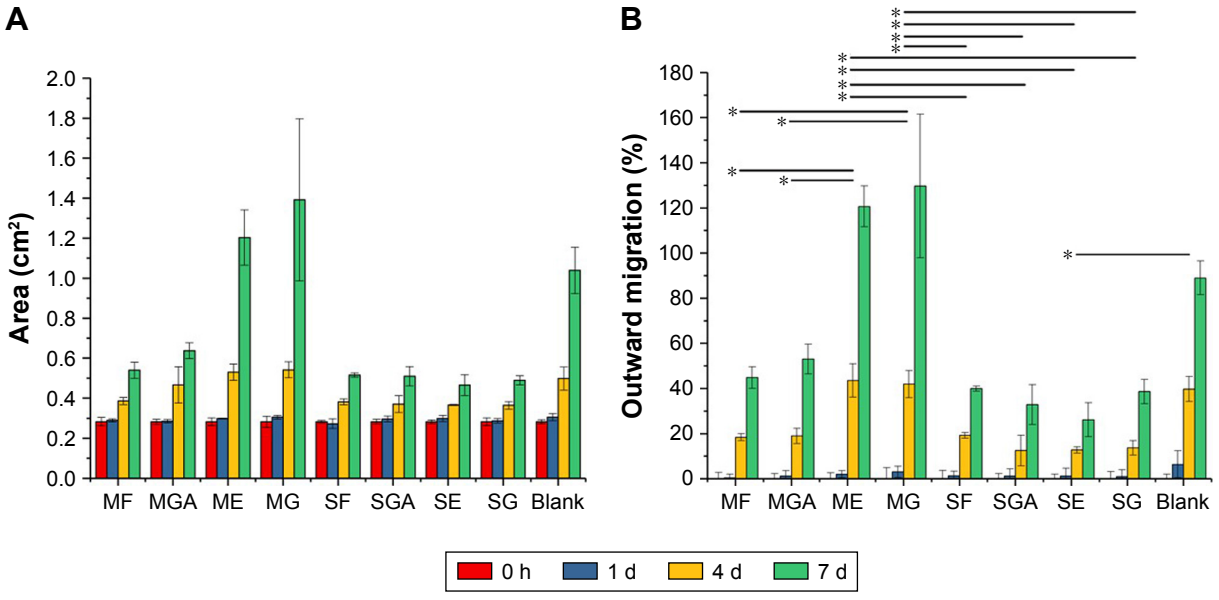

Figure 13 (**A**) Migration area of HUVECs on different membranes at designated time points (0 hour, 1 day, 4 days, and 7 days). (**B**) HUVECs migrated outward over 7 days on different membranes. *Denotes a statistically significant difference in the mean value compared with other membranes ($P<0.05$, n=3).
Abbreviations: EDC, 1-ethyl-3-(3-dimethylaminopropyl) carbodiimide; GA, glutaraldehyde; HUVECs, human umbilical vein endothelial cells; ME, mixed EDC; MG, mixed genipin; MGA, mixed GA; SE, separated EDC; SG, separated genipin; SGA, separated GA; MF, fresh mixed membranes; SF, fresh separated membranes.

because the morphology characteristics of the nanofibers are the same as that of the focal adhesion, and the amount has a high impact on cell proliferation and other behaviors.[54] Previous studies have demonstrated that vascular endothelial cells prefer smoother surfaces for adhesion and migration.[55] Mixed fibers have a smoother surface than the separated fibers. On the other hand, random orientated collagen I fibers in the separated fibers are believed to disturb the binding signal of other nanoparticles to endothelial cells.[55] This may be the reason why dense mixed nanofibers are more likely to promote HUVEC migration. In a previous study, after cross-linking, some biomolecules were activated for cell cognition. For example, after EDC/NHS cross-linking, the residual COOH and NH_2 functionalize the membranes.[51] The low cytotoxicity of genipin may facilitate HUVEC migration. Previous studies have demonstrated that genipin is an antineoplastic agent that inhibits VEGF expression.[56] However, other studies suggested that genipin-cross-linked gelatin membranes induce early angiogenesis.[57] In addition, genipin can decrease the proliferation and migration of vascular smooth muscle cells (VSMCs) in a dose-dependent manner,[58] while the overexpression of VSMC could cause stenosis.[59] Hence, genipin can maintain scaffold functions to a certain extent.

When materials are implanted into the body, the ideal biomaterials should let tissues grow gradually as the materials degrade, mimicking self-tissue. Flat fresh and cross-linked membranes were implanted under the skin of rats and removed at specific time points. Through subcutaneous implantation, the compatibility and degradation of the materials in a complex biological environment were observed. As shown in Figure 14, the host tissues infiltrated into different mats over 30 days. During the observation period, there was no obvious tissue infiltration into mixed membranes, as time elapsed. However, according to H&E staining, we found plenty of tissues that infiltrated into the separated membranes with larger pores. As time increased, the depth of tissue infiltration also gradually deepened. Laco et al[55] reported that nanofibers between 350 and 1,500 nm are involved in contact guidance in three-dimensional (3D) hydrogels. Hence, the diameter of mixed membranes might be too small for host tissue infiltration into a 3D structure. The dotted line in the figure represents the interface between the infiltrating autologous tissue and the materials. In the chemical cross-linked membranes (GA and EDC/NHS), inflammatory cells appear first and in greatest numbers. Some inflammatory cells were noted in SGA and SE. Neocapillaries were noted, indicating the tissue was regenerating. Although the infiltration of SGA was shallower than SF, SE, and SG, there was no significant difference between them. However, one problem with membranes cross-linked by GA is that they have a tendency toward calcification,[10] leading to the destruction of vascular scaffold functions. A previous study also suggested that tissue-bound aldehydes can inhibit endothelialization.[60]

Conclusion

In this study, we compared nanofibers fabricated by a mixed 10% w/v PCL/collagen (1:1) solution and a separated 10%

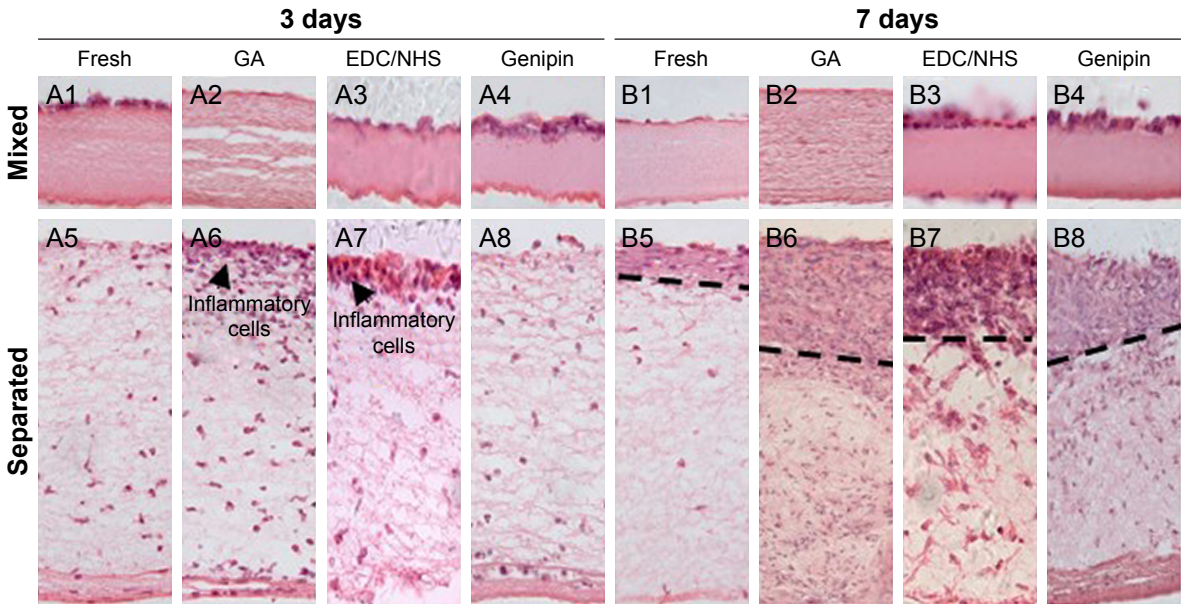

Figure 14 (*Continued*)

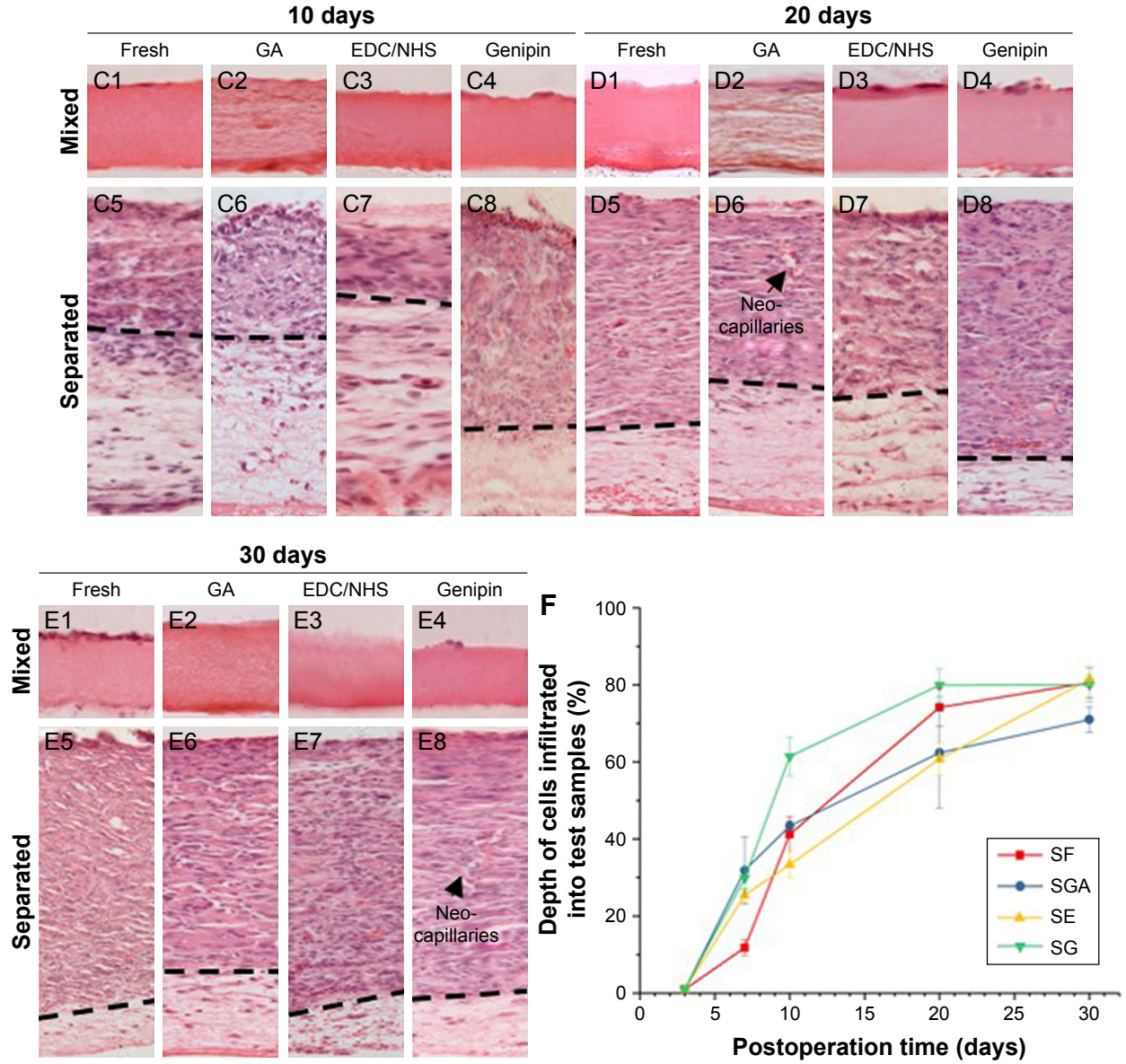

Figure 14 H&E staining images of different cross-linked membranes implanted subcutaneously at 3, 7, 10, 20, and 30 days.
Notes: Depth of the cells infiltrating into the membranes as a percentage of the depth of the test membrane. The dotted line is the boundary between the host tissue and the material. A1–A4, B1–B4, C1–C4, D1–D4 and E1–E4 are H&E staining images. F is the depth of the cells infiltrated into test samples.
Abbreviations: EDC, 1-ethyl-3-(3-dimethylaminopropyl) carbodiimide; GA, glutaraldehyde; NHS, *N*-hydroxysuccinimide; SE, separated EDC; SG, separated genipin; SGA, separated GA; MF, fresh mixed membranes; SF, fresh separated membranes.

PCL and 10% collagen solution. To enhance the structural and mechanical properties of the different membranes, GA, EDC/NHS, and genipin cross-linking technologies were adopted. By comparing the structural and mechanical properties, physical and chemical characterizations, cell compatibility, hemocompatibility, inflammatory response, and cell migration assay results, we evaluated the potential of different membranes to act as prospective vascular scaffolds that might maintain fundamental functions and promote vascular tissue development in the body. ME and MG facilitate HUVEC proliferation and migration, which helps reduce the risk of thrombosis. Although the cells had difficulty infiltrating ME and MG, these membranes maintained their mechanical properties that counteracted the impact of blood flow. Furthermore, they are hemocompatible. In conclusion, both ME and MG could be promising candidates for the development of vascular scaffolds.

Acknowledgment

This work was supported by the National Nature Science Foundation of China (grant number 81770313) and the Fund of The Pudong New District Committee of Science

and Technology (grant number PKJ2015-Y01). Dian Chen and Tonghe Zhu are co-first authors.

Disclosure

The authors report no conflicts of interest in this work.

References

1. Thurber AE, Omenetto FG, Kaplan DL. In vivo bioresponses to silk proteins. *Biomaterials*. 2015;71:145–157.
2. Roy P, Sailaja RR. Mechanical, thermal and bio-compatibility studies of PAEK-hydroxyapatite nanocomposites. *J Mech Behav Biomed Mater*. 2015;49:1–11.
3. Daelemans L, Steyaert I, Schoolaert E, Goudenhooft C, Rahier H, de Clerck K. Nanostructured hydrogels by blend electrospinning of Polycaprolactone/Gelatin nanofibers. *Nanomaterials*. 2018; 8(7):551.
4. Palchesko RN, Carrasquilla SD, Feinberg AW. Natural biomaterials for corneal tissue engineering, repair, and regeneration. *Adv Health Mater*. 2018:e1701434.
5. Ariganello MB, Simionescu DT, Labow RS, Lee JM. Macrophage differentiation and polarization on a decellularized pericardial biomaterial. *Biomaterials*. 2011;32(2):439–449.
6. Raghavan SS, Woon CY, Kraus A, et al. Human flexor tendon tissue engineering: decellularization of human flexor tendons reduces immunogenicity in vivo. *Tissue Eng Part A*. 2012;18(7–8):796–805.
7. Han F, Jia X, Dai D, et al. Performance of a multilayered small-diameter vascular scaffold dual-loaded with VEGF and PDGF. *Biomaterials*. 2013;34(30):7302–7313.
8. Neethling WM, Hodge AJ, Glancy R. Glutaraldehyde-fixed kangaroo aortic wall tissue: histology, crosslink stability and calcification potential. *J Biomed Mater Res B Appl Biomater*. 2003;66(1): 356–363.
9. Sorushanova A, Delgado LM, Wu Z, et al. The collagen suprafamily: from biosynthesis to advanced biomaterial development. *Adv Mater*. 2019;31(1):1801651.
10. Ma DH, Lai JY, Cheng HY, Tsai CC, Yeh LK. Carbodiimide cross-linked amniotic membranes for cultivation of limbal epithelial cells. *Biomaterials*. 2010;31(25):6647–6658.
11. Ratanavaraporn J, Rangkupan R, Jeeratawatchai H, Kanokpanont S, Damrongsakkul S. Influences of physical and chemical cross-linking techniques on electrospun type A and B gelatin fiber mats. *Int J Biol Macromol*. 2010;47(4):431–438.
12. Sundararaghavan HG, Monteiro GA, Lapin NA, Chabal YJ, Miksan JR, Shreiber DI. Genipin-induced changes in collagen gels: correlation of mechanical properties to fluorescence. *J Biomed Mater Res A*. 2008; 87A(2):308–320.
13. Delgado LM, Bayon Y, Pandit A, Zeugolis DI. To cross-link or not to cross-link? cross-linking associated foreign body response of collagen-based devices. *Tissue Eng Part B: Rev*. 2015;21(3):298–313.
14. Oryan A, Kamali A, Moshiri A, Baharvand H, Daemi H. Chemical crosslinking of biopolymeric scaffolds: current knowledge and future directions of crosslinked engineered bone scaffolds. *Int J Biol Macromol*. 2018;107(Pt A):678–688.
15. Sung HW, Huang RN, Huang LL, Tsai CC, Chiu CT. Feasibility study of a natural crosslinking reagent for biological tissue fixation. *J Biomed Mater Res*. 1998;42(4):560–567.
16. Mckenna KA, Hinds MT, Sarao RC, et al. Mechanical property characterization of electrospun recombinant human tropoelastin for vascular graft biomaterials. *Acta Biomater*. 2012;8(1):225–233.
17. Ye H, Zhang K, Kai D, Li Z, Loh XJ. Polyester elastomers for soft tissue engineering. *Chem Soc Rev*. 2018;47(12):4545–4580.
18. Jalaja K, James NR. Electrospun gelatin nanofibers: a facile cross-linking approach using oxidized sucrose. *Int J Biol Macromol*. 2015;73: 270–278.
19. Yin A, Zhang K, McClure MJ, et al. Electrospinning collagen/chitosan/poly(L-lactic acid-co-ε-caprolactone) to form a vascular graft: mechanical and biological characterization. *J Biomed Mater Res A*. 2013;101(5):1292–1301.
20. Kim YB, Lee H, Kim GH. Strategy to achieve highly Porous/Biocompatible Macroscale cell blocks, using a Collagen/Genipin-bioink and an optimal 3D printing process. *ACS Appl Mater Interfaces*. 2016;8(47): 32230–32240.
21. Nagarajan S, Belaid H, Pochat-Bohatier C, et al. Design of boron Nitride/Gelatin electrospun nanofibers for bone tissue engineering. *ACS Appl Mater Interfaces*. 2017;9(39):33695–33706.
22. Merkle VM, Tran PL, Hutchinson M, et al. Core-shell PVA/gelatin electrospun nanofibers promote human umbilical vein endothelial cell and smooth muscle cell proliferation and migration. *Acta Biomater*. 2015;27:77–87.
23. Sung HW, Chang Y, Chiu CT, Chen CN, Liang HC. Crosslinking characteristics and mechanical properties of a bovine pericardium fixed with a naturally occurring crosslinking agent. *J Biomed Mater Res*. 1999;47(2):116–126.
24. Torres-Giner S, Gimeno-Alcañiz JV, Ocio MJ, Lagaron JM. Comparative performance of electrospun collagen nanofibers cross-linked by means of different methods. *ACS Appl Mater Interfaces*. 2009;1(1):218–223.
25. Sung HW, Chang Y, Liang IL, Chang WH, Chen YC. Fixation of biological tissues with a naturally occurring crosslinking agent: fixation rate and effects of pH, temperature, and initial fixative concentration. *J Biomed Mater Res*. 2000;52(1):77–87.
26. Hansen P, Hassenkam T, Svensson RB, et al. Glutaraldehyde cross-linking of tendon – mechanical effects at the level of the tendon fascicle and fibril. *Connect Tissue Res*. 2009;50(4):211–222.
27. Zhang Q, Lv S, Lu J, Jiang S, Lin L. Characterization of polycaprolactone/collagen fibrous scaffolds by electrospinning and their bioactivity. *Int J Biol Macromol*. 2015;76:94–101.
28. Tsai CC, Chang Y, Sung HW, Hsu JC, Chen CN. Effects of heparin immobilization on the surface characteristics of a biological tissue fixed with a naturally occurring crosslinking agent (genipin): an in vitro study. *Biomaterials*. 2001;22(6):523–533.
29. Jin J, Song M, Hourston DJ. Novel chitosan-based films cross-linked by genipin with improved physical properties. *Biomacromolecules*. 2004; 5(1):162–168.
30. Hsieh SC, Tang CM, Huang WT, et al. Comparison between two different methods of immobilizing NGF in poly(DL-lactic acid-co-glycolic acid) conduit for peripheral nerve regeneration by EDC/NHS/MES and genipin. *J Biomed Mater Res A*. 2011;99A(4):576–585.
31. Gautam S, Chou CF, Dinda AK, Potdar PD, Mishra NC. Surface modification of nanofibrous polycaprolactone/gelatin composite scaffold by collagen type I grafting for skin tissue engineering. *Mater Sci Eng C*. 2014;34:402–409.
32. Tian Z, Wu K, Liu W, Shen L, Li G. Two-dimensional infrared spectroscopic study on the thermally induced structural changes of glutaraldehyde-crosslinked collagen. *Spectrochim Acta Mol Biomol Spectros*. 2015;140:356–363.
33. Chang MC, Tanaka J. FT-IR study for hydroxyapatite/collagen nanocomposite cross-linked by glutaraldehyde. *Biomaterials*. 2002;23(24): 4811–4818.
34. Lee H, Yeo M, Ahn S, et al. Designed hybrid scaffolds consisting of polycaprolactone microstrands and electrospun collagen-nanofibers for bone tissue regeneration. *J Biomed Mater Res B Appl Biomater*. 2011; 97B(2):263–270.
35. Safandowska M, Pietrucha K. Effect of fish collagen modification on its thermal and rheological properties. *Int J Biol Macromol*. 2013; 53:32–37.
36. Kumar B, Smita K, Cumbal L, et al. One pot phytosynthesis of gold nanoparticles using Genipa americana fruit extract and its biological applications. *Mater Sci Eng C*. 2016;62:725–731.
37. Lee SJ, Liu J, Oh SH, Soker S, Atala A, Yoo JJ. Development of a composite vascular scaffolding system that withstands physiological vascular conditions. *Biomaterials*. 2008;29(19):2891–2898.

38. Xia D, Zhang S, Hjortdal JØ, et al. Hydrated human corneal stroma revealed by quantitative dynamic atomic force microscopy at nanoscale. *ACS Nano*. 2014;8(7):6873–6882.
39. Han F, Zhang H, Zhao J, Zhao Y, Yuan X. Diverse release behaviors of water-soluble bioactive substances from fibrous membranes prepared by emulsion and suspension electrospinning. *J Biomater Sci, Polymer Ed*. 2013;24(10):1244–1259.
40. Zong X, Ran S, Kim KS, Fang D, Hsiao BS, Chu B. Structure and morphology changes during in vitro degradation of electrospun poly(glycolide-*co*-lactide) nanofiber membrane. *Biomacromolecules*. 2003;4(2):416–423.
41. Brugmans MCP, Söntjens SHM, Cox MAJ, et al. Hydrolytic and oxidative degradation of electrospun supramolecular biomaterials: in vitro degradation pathways. *Acta Biomater*. 2015;27:21–31.
42. Hass V, Luque-Martinez IV, Gutierrez MF, et al. Collagen cross-linkers on dentin bonding: stability of the adhesive interfaces, degree of conversion of the adhesive, cytotoxicity and in situ MMP inhibition. *Dent Mater*. 2016;32(6):732–741.
43. Lai JY, Ma DHK, Cheng HY, et al. Ocular biocompatibility of carbodiimide cross-linked hyaluronic acid hydrogels for cell sheet delivery carriers. *J Biomater Sci Polymer Ed*. 2010;21(3):359–376.
44. Milleret V, Hefti T, Hall H, Vogel V, Eberli D. Influence of the fiber diameter and surface roughness of electrospun vascular grafts on blood activation. *Acta Biomater*. 2012;8(12):4349–4356.
45. Asadpour S, Ai J, Davoudi P, Ghorbani M, Jalali Monfared M, Ghanbari H. *In vitro* physical and biological characterization of biodegradable elastic polyurethane containing ferulic acid for small-caliber vascular grafts. *Biomed Mater*. 2018;13(3):035007.
46. Nagai N, Nakayama Y, Nishi S, Munekata M. Development of novel covered stents using salmon collagen. *J Artif Organs*. 2009;12(1):61–66.
47. Shindo S, Motohashi S, Katsu M, Kaga S, Inoue H, Matsumoto M. Coated prostheses are associated with prolonged inflammation in aortic surgery: a cost analysis. *Artif Organs*. 2008;32(3):183–187.
48. Anderson JM, Rodriguez A, Chang DT. Foreign body reaction to biomaterials. *Semin Immunol*. 2008;20(2):86–100.
49. Imamura E, Sawatani O, Koyanagi H, Noishiki Y, Miyata T. Epoxy compounds as a new cross-linking agent for porcine aortic leaflets: subcutaneous implant studies in rats. *J Card Surg*. 1989;4(1):50–57.
50. Wang Y, Bao J, Wu X, et al. Genipin crosslinking reduced the immunogenicity of xenogeneic decellularized porcine whole-liver matrices through regulation of immune cell proliferation and polarization. *Sci Rep*. 2016;6(1):24779.
51. Pang JH, Farhatnia Y, Godarzi F, et al. In situ endothelialization: bioengineering considerations to translation. *Small*. 2015;11(47):6248–6264.
52. Hibino N, Villalona G, Pietris N, et al. Tissue-engineered vascular grafts form neovessels that arise from regeneration of the adjacent blood vessel. *Faseb J*. 2011;25(8):2731–2739.
53. Li X, Wang X, Yao D, et al. Effects of aligned and random fibers with different diameter on cell behaviors. *Colloids and Surfaces B: Biointerfaces*. 2018;171:461–467.
54. Stevens MM, George JH. Exploring and engineering the cell surface interface. *Science*. 2005;310(5751):1135–1138.
55. Laco F, Grant MH, Black RA. Collagen-nanofiber hydrogel composites promote contact guidance of human lymphatic microvascular endothelial cells and directed capillary tube formation. *J Biomed Mater Res Part A*. 2013;101A(6):1787–1799.
56. Lee SY, Kim HJ, Oh SC, Lee DH, Lee SY, Sc O. Genipin inhibits the invasion and migration of colon cancer cells by the suppression of HIF-1α accumulation and VEGF expression. *Food Chem Toxicol*. 2018;116(Pt B):70–76.
57. del Gaudio C, Baiguera S, Boieri M, et al. Induction of angiogenesis using VEGF releasing genipin-crosslinked electrospun gelatin mats. *Biomaterials*. 2013;34(31):7754–7765.
58. Jiang F, Jiang R, Zhu X, Zhang X, Zhan Z. Genipin inhibits TNF-α-induced vascular smooth muscle cell proliferation and migration via induction of HO-1. *PLoS One*. 2013;8(8):e74826.
59. Bauters C, Isner JM. The biology of restenosis. *Prog Cardiovasc Dis*. 1997;40(2):107–116.
60. Lopez-Moya M, Melgar-Lesmes P, Kolandaivelu K, de La Torre Hernández JM, Edelman ER, Balcells M. Optimizing glutaraldehyde-fixed tissue heart valves with chondroitin sulfate hydrogel for endothelialization and shielding against deterioration. *Biomacromolecules*. 2018;19(4):1234–1244.